

UC Irvine

UC Irvine Previously Published Works

Title

Groundwater and Terrestrial Water Storage [in "State of the Climate in 2010"]

Permalink

<https://escholarship.org/uc/item/5978w1kd>

Journal

Bulletin of the American Meteorological Society, 92(6)

Authors

Famiglietti, JS
Rodell, M
Chambers, DP
et al.

Publication Date

2011

Copyright Information

This work is made available under the terms of a Creative Commons Attribution License, available at <https://creativecommons.org/licenses/by/4.0/>

Peer reviewed

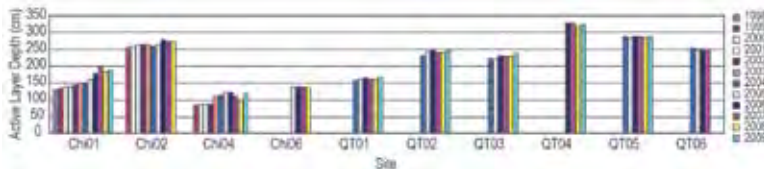


Fig. 2.29. Temporal trends in active layer depths along the Qinghai-Tibet Railway. [Modified from source: Zhao et al. (2010).]

the Northern Hemisphere for both permafrost temperatures and active layer depths. The latter respond to seasonal fluctuations in climate while changes of the deeper ground temperatures indicate long-term trends since shorter-term variations attenuate with depth. The deeper the temperatures are measured, the further back in time the surface temperature conditions they represent.

Permafrost generally warmed across the Northern Hemisphere during the past 20 to 25 years of the 20th century, and into the first few years of the 21st century (e.g., Romanovsky et al. 2007; Harris et al. 2003; Isaksen et al. 2007). Analyses of more recent data indicate that warming has generally continued. Permafrost temperatures are now up to 2°C warmer than they were 20 to 30 years ago although there are regional differences (Fig. 2.27). The overall range in permafrost temperature has decreased and is now about 1°C less than it was about 30 years ago in the polar Northern Hemisphere (Romanovsky et al. 2010b). Smaller warming rates are observed at temperatures close to 0°C compared to colder permafrost. This is especially true for ice-rich permafrost where latent heat effects dominate the ground thermal regime at temperatures close to 0°C (e.g., Romanovsky et al. 2010a; Smith et al. 2010), as well as for mountain regions in Europe where large permafrost areas are close to melting (PERMOS 2010; Haeberli et al. 2010; Isaksen et al. 2011). In European mountain permafrost, some 10-year records show a general warming trend (Isaksen et al. 2007; Haeberli et al. 2011) and permafrost temperature anomalies associated with extreme warm years (2003, 2009) have also been observed (Fig. 2.28; PERMOS 2010; Phillips et al. 2009; Zenklusen Mutter et al. 2010; Harris et al. 2003). However, trends are more pronounced in Scandinavia than in Central Europe, where only small changes or even cooling trends (Zenklusen Mutter et al. 2010) can be observed because of the strong influence of the snow cover and temperature ranges subject to latent heat effects. In the higher altitudes of Asia, ground temperatures have increased up to 0.5°C decade⁻¹ since the early 1990s, accompanied by a general increase in active layer thickness (e.g., Zhao et al. 2010; Fig. 2.29). Although

the observed trends in permafrost temperatures are consistent with changes in air temperatures, other factors such as snow cover, soil properties (including ice and moisture content), and vegetation are important factors determining the magnitude of the changes in the ground thermal regime (e.g., Haeberli et al. 2010; Romanovsky et al. 2010b).

8) GROUNDWATER AND TERRESTRIAL WATER STORAGE— M. Rodell, D. P. Chambers, and J. S. Famiglietti

Most people think of groundwater as a resource, but it is also a useful indicator of climate variability and human impacts on the environment. Groundwater storage varies slowly relative to other non-frozen components of the water cycle, encapsulating long period variations and trends in surface meteorology. On seasonal to interannual timescales, groundwater is as dynamic as soil moisture (Rodell and Famiglietti 2001; Alley et al. 2002), and it has been shown that groundwater storage changes have contributed to sea-level variations (Milly et al. 2003; Wada et al. 2010).

Groundwater monitoring well measurements are too sporadic and poorly assembled outside of the United States and a few other nations to permit direct global assessment of groundwater variability. However, observational estimates of terrestrial water storage (TWS) variations from the GRACE satellites (see Sidebar 2.2) largely represent groundwater storage variations on an interannual basis, save for high latitude/altitude (dominated by snow and ice) and wet tropical (surface water) regions (Rodell and Famiglietti 2001).

Plate 2.1i maps changes in mean annual TWS from 2009 to 2010, based on GRACE, reflecting hydroclimatic conditions in 2010. Severe droughts impacted Russia and the Amazon, and drier-than-normal weather also affected the Indochinese peninsula, parts of central and southern Africa, and western Australia. Groundwater depletion continued in northern India (Rodell et al. 2009; Tiwari et al. 2009), while heavy rains in California helped to replenish aquifers that have been depleted by drought and withdrawals for irrigation, though they are still below normal levels (Famiglietti et al. 2011). Droughts in northern Argentina and western China similarly abated. Wet weather raised aquifer levels broadly across Western Europe. Rains in eastern Australia caused flooding to the north and helped to mitigate a decade-long drought in the south. Significant reductions in TWS seen in the coast of Alaska and the

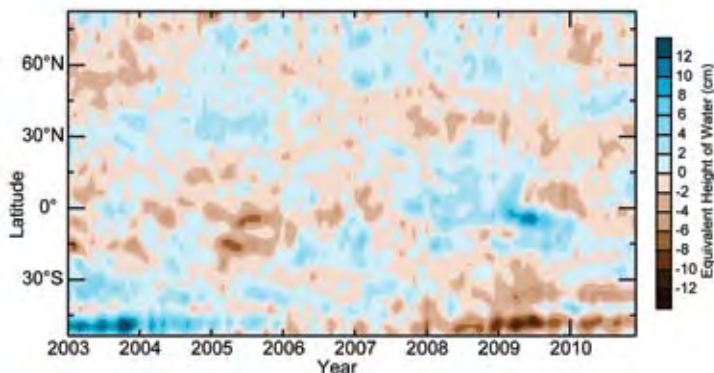


FIG. 2.33. GRACE measurements of terrestrial water storage anomalies in cm equivalent height of water by latitude. The anomalies are relative to a base period of 2003–07. Gray areas indicate regions where data are unavailable.

Patagonian Andes represent ongoing glacier melt, not groundwater depletion.

Figures 2.33 and 2.34 plot time series of zonal mean and global GRACE derived non-seasonal TWS anomalies (deviation from the mean of each month of the year) excluding Greenland and Antarctica. The two figures show that terrestrial water storage in 2010 was the lowest since 2003, though it recovered in the second half of the year. The drought in the Amazon was largely responsible, but an excess of water in 2009 seems to have buffered that drought to some extent (Fig. 2.33). The drying trend in the 25°S–55°S zone is

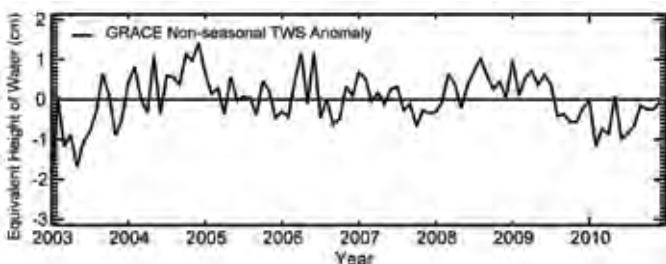


FIG. 2.34. Global average terrestrial water storage anomalies in cm equivalent height of water calculated using a 2003–07 base period.

a combination of Patagonian glacier melt and drought in parts of Australia.

9) SOIL MOISTURE—R. de Jeu, W. Dorigo, W. Wagner, and Y. Liu

In 2010, significant progress was made in consolidating globally available soil moisture datasets from a large number of ground-based stations and satellite platforms. Such harmonized datasets are essential for studying climate-related variability. Regarding the in situ component, the International

Soil Moisture Network (ISMN; Dorigo et al. 2011) was established as the successor of the renowned Global Soil Moisture Data Bank (Robock et al. 2000), which has been extensively used for climate studies. The ISMN offers a centralized system where historic and current in situ soil moisture measurements from around the world are collected, harmonized, and made available to users (see Table 2.1).

Satellite-based soil moisture estimates have significantly improved in recent years to the point where now several continental-to-global scale soil moisture products are available (e.g., Wagner et al. 2003; Njoku et al. 2003; Owe et al. 2008).

These products represent moisture conditions in the top few centimeters and depend on observation wavelength and soil wetness (Schmugge 1985; Kuria et al. 2007). Due to different observation wavelengths and retrieval methods, the quality of these products varies. Scipal et al. (2008) and Dorigo et al. (2010), using a statistical method called triple collocation, quantified satellite-based soil moisture errors in the order of $0.01 \text{ m}^3 \text{ m}^{-3}$ – $0.04 \text{ m}^3 \text{ m}^{-3}$ for the regions with a (semi) transparent vegetation cover, and $> 0.04 \text{ m}^3 \text{ m}^{-3}$ for the more densely vegetated regions. Several studies have revealed that satellite-based products are highly correlated with in situ measurements (R between 0.6 and 0.8) with root mean square errors (RMSE) ranging between $0.03 \text{ m}^3 \text{ m}^{-3}$ for semi arid regions (e.g., Africa and Australia) to $0.1 \text{ m}^3 \text{ m}^{-3}$ in France (Gruhler et al. 2010; Draper et al. 2009; Rüdiger et al. 2009).

Satellite-based soil moisture products can provide reliable estimates over sparse to moderately vegetated regions. Current satellites are not yet able to monitor soil moisture variations over densely vegetated regions (e.g., tropical rainforests) because the signals received by satellites are severely disturbed by vegetation. Over regions with snow cover and frozen soils, satellite-based microwave instruments cannot provide reliable estimates either.

The historical microwave satellites have been used to compile a consistent 20-year record of global soil moisture (Liu et al. 2009, 2011; Su et al. 2010). Satellite-based soil moisture products from both passive and active instruments were collected and harmonized in one system, covering a period since January 1991, with a spatial resolution of 0.25° and a daily time step.

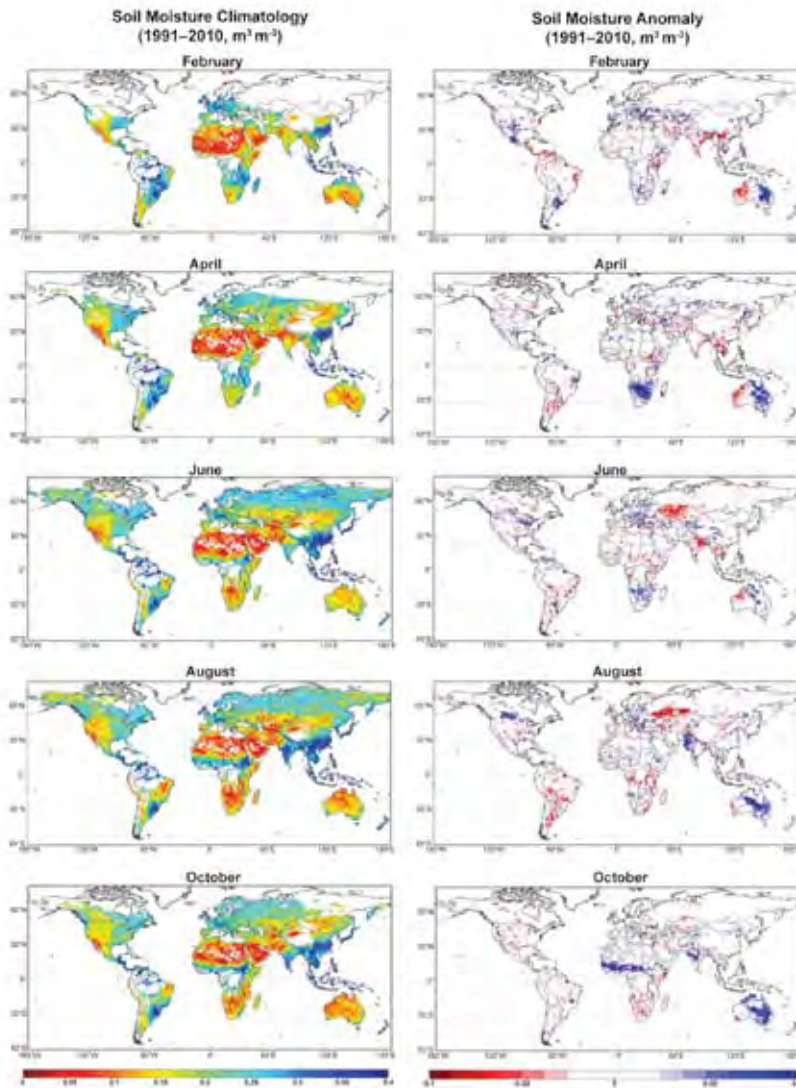


FIG. 2.35. Monthly soil moisture climatology (1991–2010) (left) and 2010 soil moisture anomaly (right) as derived from both passive and active microwave satellite sensors.

The monthly dynamics in global soil moisture are strongly driven by monsoonal circulations. During the winter phase of the monsoon, there is a low-level flow of dry, cool air from the cold continent to the warmer ocean, and precipitation over land is generally reduced. During the summer phase, there is a strong flow of atmospheric moisture from the cooler ocean to the warmer land, where the upward motion of the heated air produces the heavy rains of the monsoon season (Hastenrath 1985). These patterns are clearly visible in the soil moisture climatology (Fig. 2.35, left column). Over the Indian Peninsula, low soil moisture values between $0 \text{ m}^3 \text{ m}^{-3}$ and $0.2 \text{ m}^3 \text{ m}^{-3}$ are observed during February–April and high values between $0.2 \text{ m}^3 \text{ m}^{-3}$ and $0.4 \text{ m}^3 \text{ m}^{-3}$ are observed during August–

October. Over northern Australia, dry conditions are seen during June–August while wet conditions are seen during February–April. In Africa, the equatorial region near the Intertropical Convergence Zone is the wettest portion of the continent. Annually, the rain belt across the continent marches northward into Sub-Saharan Africa by August, then moves back southward into south-central Africa by March, resulting in wet soil moisture patterns in Sub-Saharan Africa in August and in south-central Africa in February–April.

A series of climatic events had a strong impact on the global distribution of precipitation and temperature in 2010, and these are reflected in the soil moisture anomalies (Fig. 2.35, right column). In February, both a wet (west) and dry (east) anomaly was detected over continental Australia. In April, south-central Africa was extremely wet due to excessive rainfall. In June, the first signs of the long, dry anomaly were detected over Russia and Kazakhstan. The anomaly lasted until the end of the summer. The hottest summer in Russia on record dried out a large area and led to several hundred wildfires in response (see Sidebar 7.8 for further details about this heat wave). In August, a wet anomaly was reflected over Pakistan, caused by extreme wet conditions and the additional flooding events (see section 7g3). The strong 2010 soil moisture anomalies from July onwards appear related to the oceanic phenomenon La Niña.

10) LAKE LEVELS—C. Birkett and J-F. Cretaux

Lake level as a climatic index was highlighted for the first time last year (Birkett 2010). Because lake volumes respond to changes in precipitation integrated over their catchment basins, they are indirect indicators of climatic change. The response can be seen in open lakes and reservoirs but is particularly marked for closed lakes, i.e., those having

STATE OF THE CLIMATE IN 2010

J. Blunden, D. S. Arndt, and M. O. Baringer, Eds.

Associate Eds. H. J. Diamond, A. J. Dolman, R. L. Fogt, B. D. Hall, M. Jeffries, J. M. Levy,
J. M. Renwick, J. Richter-Menge, P. W. Thorne, L. A. Vincent, and K. M. Willett



**Special Supplement to the
Bulletin of the American Meteorological Society
Vol. 92, No. 6, June 2011**



HOW TO CITE THIS DOCUMENT

Citing the complete report:

Blunden, J., D. S. Arndt, and M. O. Baringer, Eds., 2011: State of the Climate in 2010. *Bull. Amer. Meteor. Soc.*, **92** (6), S1–S266.

Citing a chapter (example):

Fogt, R. L., Ed., 2011: Antarctica [in “State of the Climate in 2010”]. *Bull. Amer. Meteor. Soc.*, **92** (6), S161–S171.

Citing a section (example):

Wovrosh, A. J., S. Barreira, and R. L. Fogt, 2011: [Antarctica] Circulation [in “State of the Climate in 2010”]. *Bull. Amer. Meteor. Soc.*, **92** (6), S161–S163.